CHAPTER II
LITERATURE REVIEW

2.1 Carbon Dioxide (CO_2) and Climate Change

Carbon dioxide is a greenhouse gas (GHG) which is the most impact on climate change. Other GHGs include water vapor (H_2O), carbon dioxide (CO_2), methane (CH_4), nitrous oxide (N_2O) and ozone (O_3). These GHGs have different global warming potential, as shown in Table 2.1 Using CO_2 as a baseline, other GHGs have stronger effects of the global warming potential than CO_2 but they are presented in very much smaller quantities than CO_2. Therefore, carbon dioxide is the major greenhouse gas that receives much attendance regarding the global warming (Larson *et al.*, 2011).

Table 2.1 Global warming potential over 100 years on a per molecule basis* (Larson *et al.*, 2011)

Types of GHGs	GWP*
Carbon dioxide (CO_2)	1
Methane CH_4 (ppb)	25
Nitrous oxide N_2O (ppb)	298
HFC-134a CF_3CH_2F (refrigerant)	1430
Carbon tetrachloride CCl_4	1400
CFC-12 CF_2Cl_2 (refrigerant)	10900
Sulphur hexafluoride SF_6	22800

*Units are Global Warming Potential (GWP), a unit relative to the amount of warming from the same mass of CO_2.

Carbon dioxide is generated by different ways, such as natural, anthropogenic processes and activities. Nowadays, the trend of energy consumption increase rapidly, especially in the electricity generation, transportation and industrial activities. These activities have led to the increase in the emission of CO_2 to the atmosphere (Larson *et al.*, 2011). Figure 2.1 predicts the trend of global CO_2 emissions during the period 1980-2050. For the trend of energy consumption, all sectors increase their CO_2 emission to the atmosphere but the largest sector of CO_2 emission is the power generation (Marchal *et al.*, 2011). In the future, European strategic energy technologies plan to reduce 20 percent of the greenhouse gas emissions by 2020 and to reduce 50% of the greenhouse gas emissions by 2050 (Casco *et al.*, 2014).

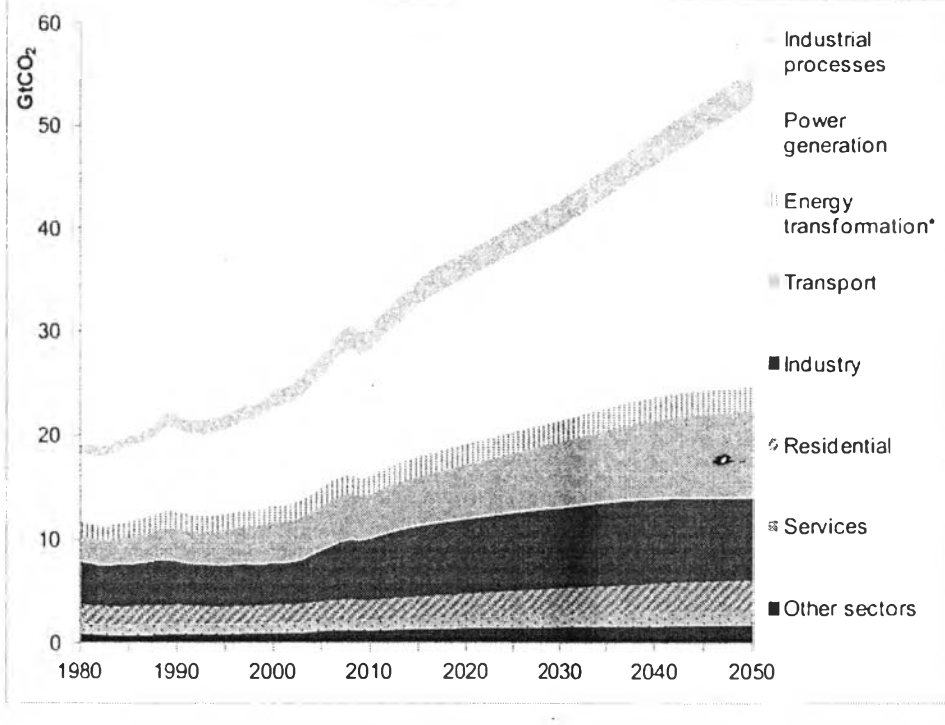

Figure 2.1 Global CO_2 emissions by source: *Baseline*, 1980-2050 (Marchal *et al.*, 2011).

Note: The category "energy transformation" includes emissions from oil refineries, coal and gas liquefaction.

2.2 CO_2 Capture and Separation

CO_2 capture and storage (CCS) is the process involving with capturing and underground storing a large amount of industrial CO_2 emissions. Nowadays, the development of CO_2 capture focuses on the power regeneration systems which consume over 50 percent of all energy sources leading to produce high CO_2 concentration to atmosphere. However, there are other CO_2 emission sources which include iron and steel manufacturing, cement production, refineries, petrochemical and other industries, and fossil fuel production. Owing to the attempt to reduce the CO_2 emissions to the atmosphere, the CO_2 capture and storage (CCS) has become the interest. In addition, the technologies for capturing CO_2 can be categorized into three main groups which include post-combustion, oxy-fuel combustion and pre-combustion (Larson *et al.*, 2011) as shown in Figure 2.2.

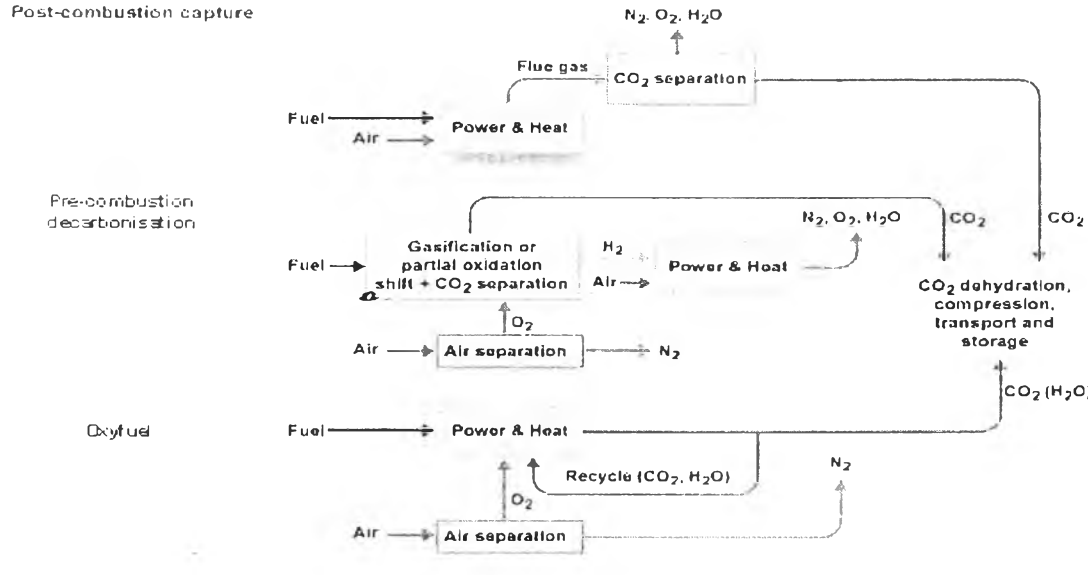

Figure 2.2 The different routes for CO_2 capture and separation (CCS Masters, 2014).

2.2.1 Post-combustion

The main idea of post-combustion is to separate CO_2 from the flue gases which are produced from combustion of fuel with air at atmospheric pressure.

However, there are many industries where use the post-combustion process for capturing CO_2 such as coal-fired power stations, the steel and cement industries, and refineries furnace because these industries use air or the stream from their processes to burn the fuel. In addition, CO_2 emission from this type of combustion is very low in partial pressure due to the condition is operated at atmospheric pressure (Larson *et al.*, 2011).

Table 2.2 Advantages and disadvantages of post-combustion

Advantages	Disadvantages
• Capture technologies are available which are proven at pilot scales. • Flexibility in switching between capture/no capture	• Energy requirements • The size of the equipment

2.2.2 Pre-combustion

The CO_2capture of pre-combustion occurs during the process before burning of fossil fuels or biomass in a combustor. This process can be coupled with producing hydrogen and, hence, it can be called as a hydrogen production with CO_2 removal. In addition, pre-combustion processes can be used to generate syngas and CO_2 can be captured at the same (Larson *et al.*, 2011).

Table 2.3 Advantages and disadvantages of pre-combustion

Advantages	Disadvantages
• Lower compression cost than post-combustion • Low SO_X and NO_X emissions • The main product is syngas.	• The feed fuel must be converted to syngas first. • Gas turbines, heaters, and boilers must be modified for hydrogen firing.

2.2.3 Oxy-fuel Combustion

Oxy-fuel combustion involves with combustion of fuel with pure oxygen to produce CO_2 and H_2O. Then, the H_2O is removed by lowering the temperature and condensing out. However, the air combustion is a problem that should be avoided. This problem occurs when there is high amount of nitrogen in the process because the nitrogen component is not heated and led to reduce the fuel combustion (Larson *et al.*, 2011).

2.3 Adsorption

Adsorption technique is used to capture CO_2 by adsorbent. Adsorption process occurs at the interface where CO_2 molecules in the gas stream, e.g. flue gas, attach on the adsorbent surface. Then, CO_2 molecules are absorbed by physical forces or chemical bonds at adsorption conditions while the rest of, the flue gases are passed through the adsorbent as shown in Figure 2.3.

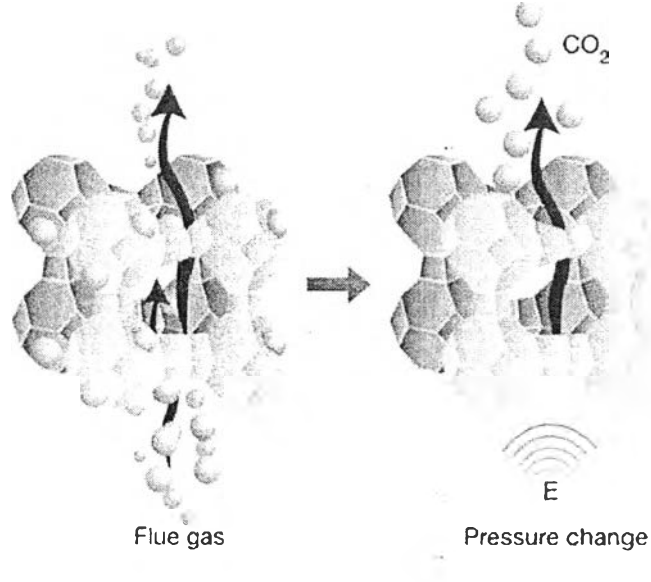

Figure 2.3 The CO_2 adsorption behavior on the adsorbent surface (Mclnerney, 2014).

After the adsorption process, CO_2 molecules are removed from the adsorbent by a desorption process which occurs when temperature or pressure is changed (Cook, 2012). Comparing to absorption where amines are commonly used as absorbents, the adsorption process is effective over the absorption process in terms of low cost material, lower energy consumption for regeneration and no corrosion problem (Casco *et al.*, 2014). However, there are several techniques employed in the adsorption/desorption process which include thermal swing adsorption (TSA), vacuum swing adsorption (VSA), pressure swing adsorption (PSA) and electrical swing adsorption (ESA).

2.3.1 Thermal Swing Adsorption (TSA)

This technique is able to removed CO_2 from the adsorbent at high temperature condition by using steam or hot CO_2 for heating the adsorbent (Plaza *et al.*, 2013).

2.3.2 Vacuum Swing Adsorption (VSA)

This technique is able to adsorb CO_2 at the pressure above atmospheric pressure and to remove CO_2 at reducing pressure below atmospheric pressure (Plaza *et al.*, 2013).

2.3.3 Pressure Swing Adsorption (PSA)

This technique is similar to VSA which is able to adsorb CO_2 at the pressure above atmospheric pressure but CO_2removal at reducing pressure close to atmospheric pressure (Plaza *et al.*, 2013).

2.3.4 Electrical Swing Adsorption (ESA)

This technique uses the Joule effect which is used to remove CO_2 by applying a voltage to heat the adsorbent (Plaza *et al.*, 2013).

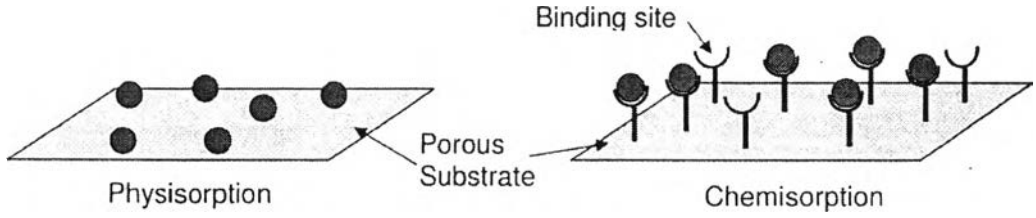

Figure 2.4 The physisorption of CO_2 and the chemisorption of CO_2 on porous substrate (Berger and Bhown, 2011).

The adsorption mechanisms can be classified into two types which include physisorption and chemisorption. In physisorption, the CO_2molecules are adsorbed on the porous substrate by van der Waals forces. The heat of adsorption of this process is low and it is just slightly greater than the heat of sublimation of the adsorbate. These results of the low interaction forces exhibit low CO_2 adsorptions, e.g. only 25 to -40 kJ/mole for the heat of CO_2 adsorbed on activated carbon sorbent. In addition, Plaza *et al.* (2008) supported that a commercial activated alumina could be only adsorbed CO_2 molecules by physisorption. However, the adsorbent can be modified by some reactive sites such as amine functions which have a much higher heat of adsorption. The heat of adsorption of adsorbent modified with amine can range between -60 and -100 kJ/mole, depending on types of amine used. Moreover, the low heat of adsorption will reduce the energy consumption for desorption process (Berger and Bhown, 2011). There are some drawbacks of physisorbents such as activated carbon and zeolite when water is present in the feed gas. This effect leads to the reduction of the CO_2 adsorption capacities. In zeolite, it is a highly polar adsorbent with high H_2O selectively over CO_2. Therefore, the process of water removal is necessary before capturing CO_2 (Lee *et al.*, 2007).

In chemisorption, the CO_2 molecules are interacted with the binding sites on porous substrate by creating the covalent bonds with a much greater heat of adsorption, equal to the heat of reaction (Berger and Bhown, 2011). Alumina modified with primary and secondary amines can form carbamates that indicate higher CO_2 capture capacity than unmodified alumina (Plaza *et al.*, 2008). Furthermore, there are several new chemisorbents which have been synthesized such as potassium carbonate pro-

moted hydrotalcites, sodium oxide doped alumin as and lithium zirconate (Lee *et al.*, 2007). The difference between physisorption and chemisorption is shown in Table 2.4.

Table 2.4 Comparison between physisorption and chemisorptions (Amrita, 2014)

Physisorption	Chemisorption
Low heat of adsorption usually in the range of 20-40 kJ mol^{-1}	High heat of adsorption in the range of 40-400 kJ mol^{-1}
Force of attraction are Van der Waal's forces	Forces of attraction are chemical bond forces
It usually takes place at low temperature and decreases with increasing tempera-ture	It takes place at high temperature
It is reversible	It is reversible
It is related to the ease of liquefaction of the gas	The extent of adsorption is generally not related to liquefaction of the gas
It is not very specific	It is highly specific
It forms multi-molecular layers	It forms monomolecular layers
Not require any activation energy	Require activation energy

2.4 Porous Materials

The porous material is a rigid structure containing many pores. They can be adapted in various applications, such as catalyst support, gas separation, water purification, electrode material for energy storage devices, adsorbent, molecular sieves, thermal insulation, etc. (Chaisuwan, 2011). According to IUPAC, the pore size of porous material can be classified into three categories which include micrporous, mesoporous, and macroporous.

- Microporous: A material is containing pores with diameters smaller than 2 nm.
- Mesoporous: A material is containing pores with diameters between 2 nm and 50 nm.
- Macroporous: A material is containing pores with diameters larger than 50 nm.

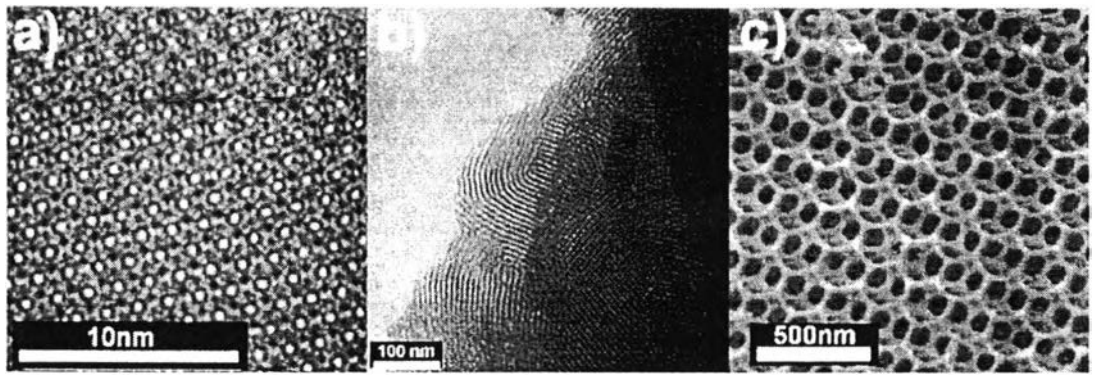

Figure 2.5 a) A microporous material, b) A mesoporous material, and c) A macroporous material (Polarz and Smarsly, 2002).

The surface area of porous material has become an important factor for the transfer of molecules. Polarz and Smarsly (2002) showed that the pores might be filled by any matter that came from the difference surrounding network. In addition, the ordered porous materials are attractive in terms of control over pore sizes and pore shapes. These results seem to be a homogeneous material which performs selectively to adsorb a small molecule (such as CO_2 molecule) from the mixture containing molecules (such as 14 % CO_2 in N_2) (Davis, 2002). On the other hand, the disordered porous materials exhibit wide ranges of pore sizes and the shapes of pores are irregular. Therefore, the distribution of sizes, shapes and volumes of voids spaces in the porous materials are important to the specific application used. Figure 2.6 exhibits that the types of pores can be classified into four types which are closed pores (a), open pores (b, c, d, e, f), blind pores (b, f) and interconnected pores (e). There are

five shapes of pores which are cylindrical open (c), cylindrical blind (f), ink bottle shaped (b), funnel shaped (d) and roughness (g).

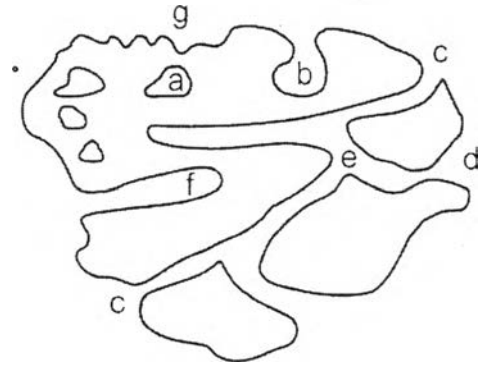

Figure 2.6 The different types of pores (Norby, 2014).

Currently, the porous materials are rapid developed in the nanoporous materials which indicate high performance in CO_2 capture application. These materials are focused on microporous and mesoporous materials.

The effect of pore size using amine-modified ordered mesoporous silica for CO_2 capture was studied by Zeleňák *et al.* (2008). In their work, three different types of mesoporous silica materials were prepare from MCM-41 (pore size 33Å; 2D structure), SBA-12 (pore size 38Å; 3D structure) and SBA-15 (pore size 71Å; 2D structure) and functionalized with aminopropyl (AP) ligands in order to enhance the CO_2 capture. The transmission electron microscopy (TEM) characterized that the pore size diameters of MCM-41, SBA-12 and SBA-15 were 3 nm, 3.5 nm and 7.5 nm. respectively. These TEM results are in agreement with the data provided by BET surface area. In case of SBA-15 functionalized with aminopropyl, it had the highest CO_2 adsorption capacity of 1.50 mmol/g at 25 °C and 1 atm due to the highest amine functional groups on its surface. These basic amine sites could interact with acidic CO_2 molecules to enhance the CO_2 adsorption capacity by the chemisorption. In case of SBA-12 could quickly adsorb CO_2 comparing to MCM-41 and SBA-15 because its pore structure was a three-dimensional mesoporous material which had a high amount of amine sites over MCM-41 and SBA-15.

The narrow pore size distribution with using nanoporous carbons for CO_2 capture was studied by Meng and Park (2012). In their work, the nanoporous carbons were prepare from thermoplastic acrylic resin and MgO powder carbonized at 500, 700, 800, 900 and 1000 °C. After carbonization, the pore structures of nanoporous carbons exhibited large amount of narrow micropores and mesopores because the carbonization increased the carbon content in their structure. In addition, the thermoplastic acrylic resin was decomposed during carbonization to form crystallography on the surface of MgO. As increasing the carbonization temperature, the surface area increased from 237 to 1251m^2/g and the total pore volume increased from 0.242 to 0.763cm^3/g due to high amount of volatiles removal from the materials that affected to the porosity of their structure. The effect of CO_2 adsorption after carbonization at 900 °C demonstrated the highest CO_2 adsorption capacity at 194 mg/g (4.41 mmol/g) at 1 bar and 25 °C owing to high micropore volume.

The effects of pore size, pore volume and the loading weight on the separation performance with using SBA-15/CMS as a membrane were reported by Tseng *et al.* (2013). Firstly, the SBA-15 fillers were prepared by using different aging temperature at 90, 100, 110 and 120 °C to study the effect of pore size, surface area, total pore volume and shape of particle on their structure. The results indicated that the particle size, the diameter and pore size increased with increasing aging temperature and the ordered mesoporous SBA-15 silica showed at the highest aging temperature of 120 °C. In case of the surface area and total pore volume decreased when the aging temperature was increased from 100 to 120 °C owing to the reduction in the micropore and mesopore structure. The effect of particle shape was not changed when the aging temperature was increased and the shape was a long hexagonal pillar-shaped. As the degree of crystallinity (T_g) of PPO polymer and SBA-15 composite membranes increased with increasing aging temperature due to covalent crosslinking. This result supported that there are more Si-O and Si-O-Si groups on the SBA-15 surface. Thus, the pore size of mesopore and macropore was better to remove PPO into the SBA-15 channels. The effect of SBA-15 was varied at 0.025, 0.05, 0.1, 0.2 and 0.4 wt%. The result showed that T_g of the composite membranes increased with increasing loading of SBA-15 to 0.1 wt%. As the increasing loading of SBA-15 from 0.1 to 0.4 wt%, T_g of the composite membranes decreased. For gas separation,

the composite membrane was selective for the transport of H_2 and CO_2 over CH_4 at 100 °C of the aging temperature and at 0.025 wt% of SBA-15 loading. As the aging temperature increased from 110 to 120 °C, the selectivity of H_2 and CO_2 decreased because the larger pore size could not be shrunk enough to achieve size selectivity.

The effects of carbon nanopore size and surface oxidation for CO_2 capture from a mixture of CO_2/ CH_4 were evaluated by Furmaniak *et al.* (2013). The CO_2 adsorption efficiency depended on two factors which are the adsorbent structure and the dispersion of functional groups on the surface. In their work, the pore size distributions of virtual porous carbon (VPC) samples were investigated by using geometrical method of Bhattacharya and Gubbins (BG). Each VPC sample had a different number of carbon components which were microporous materials. The results indicated that the uniform pores and the small carbon nanopores found in case of a high number of carbon components. The effect of adsorption identified that adsorbent with narrow pore diameters could adsorb large amounts of both CO_2 and CH_4 molecules because molecules could be easily accessible in nanopores. In case of surface oxidation, the presence of carbonyl functional groups showed high adsorbed CO_2 over CH_4 because CO_2 molecules had stronger electrostatic interactions with carbonyl groups than CH_4. These results showed that the surface functionalities had more important effect on CO_2/CH_4 separation than porosity. In addition, the high pressure adsorption encouraged the adsorption of CO_2/CH_4 mixtures at low CO_2 concentration.

The effect of pore structure of support using three-dimensional molecular basket sorbent (3-D MBS) for CO_2 capture was also studied by Wang *et al.* (2014). In their work, 3-D MBS samples were prepared by loading PEI on mesocellular siliceous foam (MCF), hexagonal mesoporous silica (HMS) and MSU-J. The CO_2 adsorption performances of 3-D MBS samples were compared with the other samples which included carbon black (CB), SBA-15 and MCM-41. Before loading PEI, the MCF and CB had larger pore volume than other samples but their structures were quite different. In MCF sample, the pore structure was 3-D spherical. In CB samples, the pore structure was disordered. After loading PEI, the 3-D MBS samples (MCF, HMS and MSU-J) exhibited higher PEI loading than CB, SBA-15 and MCM-4 due to higher surface area. In case of the CO_2 adsorption performance, the MCF with 65

wt% PEI loading showed the highest CO_2 adsorption capacity because MCF was 3-D mesoporous material with uniform spherical pore interconnected.

2.5 Adsorbent

An adsorbent can adsorb CO_2 molecules in two different ways. Firstly, CO_2 molecules are adsorbed via physisorption by van der Waals forces. Secondly, CO_2 molecules are adsorbed via chemisorption by covalent bonding with basic sites on the surface of an adsorbent. Nowadays, there are several types of adsorbents which most commercial adsorbents can be classified into three classes which include:

- Oxygen Containing Compounds: An adsorbent has hydrophilic and polar such as silica gel and zeolite.
- Carbon-based Compounds: An adsorbent has hydrophobic and non-polar such as activated carbon and graphite.
- Polymer-based Compounds: An adsorbent has polar or non-polar functional groups in a porous structure.

Other types of adsorbents include calcium oxides, hydrotalcites, lithium zirconate, and organic-inorganic hybrids (Choi *et al.*, 2009). In the present work, we will focus on the polymer-based compound. However, the important factors are used to enhance the performance of CO_2 adsorption capacity depending on the adsorbent used, such as uniform pore, large surface area (high physisorption), small pore size (nanopores ranging in size from 2-50 nm), selectivity and high numbers of basic sites on the surface of an adsorbent (high chemisorption). Table 2.5 indicates the properties of each commercial porous adsorbent that are the important parameters to select the adsorbent for capturing CO_2 (Singh and Kaushal, 2013). Moreover, an adsorbent can be improved by the presence of heteroatoms such as nitrogen and oxygen. For instance, the functionalized nitrogen atoms on the surface of an adsorbent exhibit an increasing number of basic groups (Drage *et al.*, 2007).

Table 2.5 Representative properties of commercial porous adsorbents (Singh and Kaushal, 2013)

Adsorbent	Nature	Pore Diameter (d_p), Å	Particle Porosity, E_p	Particle Density (p_p), cm^3/g	Surface (s), m^2/g	Capacity for H_2O Vapor at° 25 °C and 4.6 mmHg, wt% (Dry Basis)
Activated alumina	Hydrophilic amorphous	10-75	0.5	1.25	320	7
Silica gel:						
Small pore	Hydrophilic amorphous,	22-26	0.47	1.09	750-850	
Large pore	Hydrophobic amorphous	100-150	0.71	0.62	300-350	
Activated carbon:						
Small pore	Hydrophilic amorphous,	10-25	0.4-0.6	0.5-0.9	400-1200	1
Large pore	Hydrophobic amorphous	>30	-	0.6-0.8	200-600	-
Molecular-sieve carbon	Hydrophobic	2-10	-	0.98	400	-
Molecular-sieve zeolites	Polar-hydrophilic, crystalline	3-10	0.2-0.5	1.4	600-700	20-25
Polymeric adsorbents	-	40-25	0.40-0.55	-	80-700	-

2.5.1 Silica

Silica is an amorphous porous material in the form of silicon dioxide (SiO_2) such as M41S, Santa Barbara Amorphous (SBA-n), anionic surfactant template mesoporous silica (AMS), etc. These types of adsorbents have several advantages for capturing CO_2 such as high surface area, high pore volume, small pore size and good thermal stability (Yu *et al.*, 2012). Moreover, the silica can be used to enhance the CO_2 adsorption capacity by various methods such as designed the size of pores, impregnation with amine groups on the surface of silica, etc.

The effects of CO_2 adsorption properties using amine-modified mesocellular silica foam as an adsorbent were studied by Yan *et al.* (2011). In their previous work, they studied the CO_2 adsorption performance on amine impregnated SBA-15 as an adsorbent. The results indicated that amine loading had a direct effect on the

size of pore volume which large pore volume exhibited a high CO_2 adsorption capacity. In their present work, mesocellular silica foam (MCF) substrates were prepared with different window sizes (M-F0, M-F3 and M-F6) by using the method of Schmidt-Winkeland the MCF substrates were impregnated with different PEI loading by wet impregnation method. After loading with 50 wt% of PEI, surface area and total pore volume of M-F0 sample decreased from 811 and 1.51 m^2/g to 16.5 and 0.10cm^3/g, respectively because PEI filled in the mesopores of silica. However, the CO_2 adsorption capacity increased from 0.33 to 2.63 mmol-CO_2/g-adsorbent due to chemisorption with the amine groups. When PEI was loaded beyond 50 wt%, the effect of CO_2 uptake was decreased because of less contact area. Furthermore, the window sizes (diameter of pore that connect the cells) of M-F0, M-F3 and M-F6 are 5.0, 8.6 and 11.3 nm, respectively. These different window sizes of MCF substrates demonstrated the same cell diameter (diameter of spherical pore), i.e. 23 nm. For the effect of CO_2 adsorption, the M-F6/50 wt% of PEI (3.45 mmol/g of adsorbent) was slightly higher CO_2 uptake thanM-F3/50 wt% (3.37 mmol/g of adsorbent) under 5% CO_2 in N_2 at 75 °C. After 8 cycles of adsorption-desorption, M-F6 / 50 wt% of PEI indicated a good property for CO_2 adsorption.

The effects of adsorption temperature and pentaethylenehexamine (PEHA) loading with using on mesoporous silica support as an adsorbent for CO_2 capture form simulated flue gas were studied by Wei *et al.* (2013). In their work, an adsorbent was prepared by loading PEHA on SBA-15 by wet impregnation method with different PEHA loadings at 0, 15, 30, 50 and 70 wt%. The results showed that the surface area and pore volume of the silica support decreased continuously with increasing of PEHA loadings because PEHA filled in the pore of silica, thus, reducing the surface area. From TGA diagram, SBA with PEHA loading showed two peak of mass loss. The first peak was mass loss from desorption of adsorbates. The second peak was mass loss from volatilization of PEHA. For the effect of CO_2 adsorption, SBA-15 with PEHA loading gave higher CO_2 uptake than the unmodified SBA-15 and the CO_2 adsorption capacity increased with increasing PEHA loading because basic amine groups on the surface of support could interact with acidic CO_2 molecules and the reaction equations are shown in Equations 2.1 and 2.2.

Reaction equations:

$$CO_2 + 2RNH_2 \leftrightarrow [RNH_3]^+ [O\text{-}\overset{\overset{O}{\|}}{C}\text{-}\overset{\overset{H}{|}}{N}\text{-}R]^- \quad (2.1)$$

$$CO_2 + 2R_2NH \leftrightarrow [R_2NH_2]^+ [O\text{-}\overset{\overset{O}{\|}}{C}\text{-}\overset{\overset{R}{|}}{N}\text{-}R]^- \quad (2.2)$$

At low PEHA loading, PEHA-SBA-15 showed a low CO_2 uptake because the small amine groups interacted with the silanol groups. At high PEHA loading, the CO_2 adsorption capacity of PEHA-SBA-15 increased because a greater amount of amine groups could interact with CO_2 molecules. The CO_2 adsorption capacity of SBA-15, SBA-15-PEHA-15, SBA-15-PEHA-30, SBA-15-PEHA-50 and SBA-15-PEHA-70 were 7.0, 21.7, 76.8, 154.2 and 201.7 mg of CO_2/g of adsorbent, respectively. For SBA-15-PEHA-50, the effect of adsorption temperature was studied at temperature from 25 to 125 °C. These results indicated that the highest CO_2 adsorption capacity was 3.50 mmol of CO_2 /g of adsorbent at 80°C owing to the optimal control temperature for CO_2 adsorption.

2.5.2 Activated Carbon

Activated carbon is a high porous material which can be produce from many sources such as bituminous coal, petroleum coke, peat, coconut shells and wood. The activation processes can be divided into two methods which are steam activation and chemical activation (Venkatesan, 2013).

2.5.2.1 Steam Activation

There are two steps to manufacture activated carbon which are carbonization and activation. For the carbonization step, the raw materials are heated at the temperatures of 400–500 °C under an oxygen free atmosphere in order to remove the volatile matters. For the activation step, the carbonized materials are activated by steam or carbon dioxide at 800–1000 °C.

The preparation of an activated carbon from black liquor lignin by physical activation using steam for methylene blue removal was reported by Fu *et al.* (2013). In their work, the activated carbons were prepared from two steps

which were carbonization under an oxygen free atmosphere and activation with using steam. In the preparation of activated carbons, there were several parameters that had been investigated, such as carbonization temperature, activation temperature, carbonization time, and activation time. The results indicated that the optimized lignin based activated carbon (LCA) was observed at a carbonization temperature of 450 °C, a carbonization time of 60 min, an activation temperature of 725 °C, and an activation time of 40 min. For the effect of carbonization, the temperature of 450 °C was suitable for the production of LCA because it exhibited the highest BET surface area of 288.79 m^2/g and the carbonized time for 60 min was performed to completely eliminate the volatile matter. For the effect of activation, the temperature of 725 °C performed the highest BET surface area of 310.15 m^2/g (carbonized at 450 °C for 60 min, activated for 40 min) and the activated for 40 min allowed pore open in gas it was performed by increasing of the BET surface area. In case of methylene blue (MB) adsorption, LCA exhibited the maximum MB adsorption capacity at 92.51 mg/g as it showed better result than other adsorbents.

2.5.2.2 Chemical Activation

The raw materials are impregnated with a strong dehydrating agent such as phosphoric acid or zinc chloride. Then, it is heated at the temperature of 500–800 °C in order to activate the carbon. After that, the activated carbon is washed, dried and ground to receive the powder. Fu *et al.* (2013) described that an activated carbon from this method demonstrated the ability to form a high specific area and a high pore volume. However, this method showed some drawbacks such as the production of byproducts, using complex procedures, high energy consumption for activation process, and high maintenance costs due to corrosion of equipment.

The preparation of large surface area activated carbon from stone biomass by chemical activation with using phosphoric acid was studied by Danish *et al.* (2014). In their work, they studied several parameters for the preparation of an activated carbon such as activating agent concentration and activation temperature. For the effect of activating agent concentration, different concentration was studied from 1.7 wt% to 50 wt% which a result of surface area increased from 216 m^2/g to1214 m^2/g, respectively. This surface area showed a continuous increase with an activating agent concentration because the activating agent was allowed to

create new pores in the biomass structure by releasing small molecules during the chemical activation process. Above 50 wt% of H_3PO_4 concentration, this result showed the decrease of surface area due to the reduction in pore volume. For the effect of activation temperature, the temperature was studied in range of 400 °C to 900 °C. When the temperature increased to 900 °C, the product yield decreased from 64.7 % to 24.9 %, while the surface area performed increased from 240 m^2/g to 1240 m^2/g. Therefore, the optimized stone biomass based activated carbon was observed at a phosphoric acid concentration of 50 wt%, an activation temperature of 900 °C and an activation time of 120 min. This result showed the surface area over 1000 m^2/g with compromising yield.

An activated carbon has several advantages for capturing CO_2 such as high abrasion resistance, high thermal stability, high surface area (in the range of 300-4000 m^2/g), large pore volume and small pore diameter. However, it has a drawback that an activated carbon can react with oxygen at moderated temperature (above 300 °C) (Singh and Kaushal, 2013).

In order to improve properties of the adsorbent for CO_2 capture, considerable synthetic effort to develop pore sizes of adsorbent, one of the well-developed activated carbon is modified in mesoporous materials forms. Another way to enhance the CO_2 adsorption performance with using the impregnation of amine groups on the surface of an adsorbent.

A potential source of basic sites for CO_2 capture by using different amine group compounds for impregnation and using commercial activated carbon as a support was evaluated by Plaza *et al.* (2007). A series of sorbents were obtained by filling in activated carbon (AC) with different amine group compounds which included diethylentriamine (DETA), pentaethylenehexamine (PEHA), and polyethylenimine (PEI) (as shown in Figure 2.7) by a wet impregnation method. The results revealed that AC-DETA showed the highest amount of nitrogen up to 14 %, even though amine loading of DETA was the lowest compare with PEHA and PEI. The BET surface area of untreated AC, AC-DETA, AC-PEHA and AC-PEI was shown at 1762, 157, 170 and 90 m^2/g, respectively. The BET surface area of impregnated activated carbons exposed the reduction of adsorption area due to the pore blocking effect. Therefore, the CO_2 adsorption capacity of untreated activated carbon exhibited

the highest CO_2 adsorption of 1.61 mmol/g at ambient condition. However, the CO_2 adsorption capacity of AC-DETA at high operating temperature performed higher CO_2 adsorption capacity than untreated activated carbon due to the highest nitrogen content.

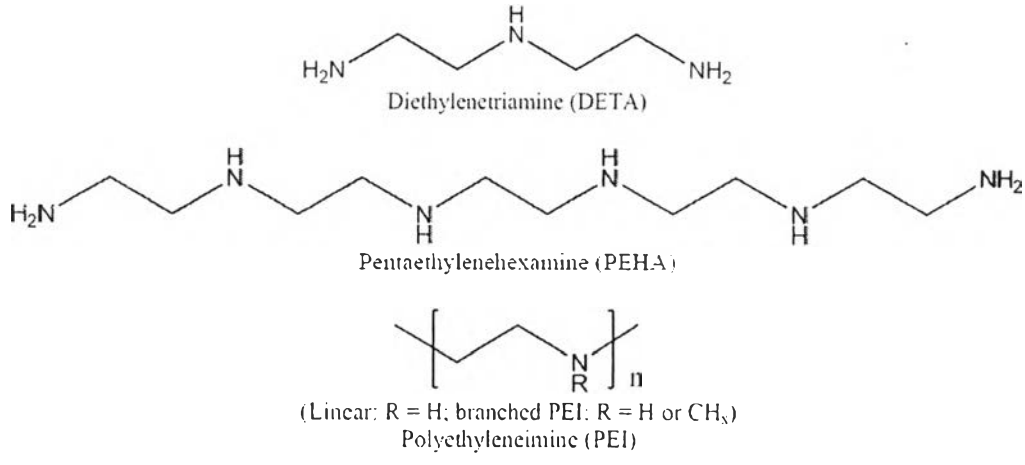

Figure 2.7 The structure of DETA, PEHA and PEI (Yu *et al.*, 2012).

A potential source of basic sites for CO_2 capture by using different amine group compounds for impregnation and using commercial alumina as a support was evaluated by Plaza *et al.* (2008). A series of sorbents were obtained by filling in activated carbon with different amine group compounds which included diethylenetriamine (DETA), diisopropanolamine (DIPA), triethalnolamine (TEA), 2-amino-2-methyl-1,3-propanediol (AMPD), pentaethylenehexamine (PEHA), and polyethyleneimine (PEI) as shown in Figures 2.7 and 2.8. These amine compounds were loaded on the support by a wet impregnation method. After impregnation with amine compounds, the nitrogen and carbon contents of sorbents increased due to the distribution of amine groups on the surface of supports; whereas, the oxygen content of the amine group compounds impregnated solid sorbents (A-DIPA, A-AMPD and A-TEA) increased double as compare to the amine group compounds impregnated solid sorbents (A-DETA, A-PEHA and A-PEI) because their structures consisted of hydroxyl functional groups. The CO_2 adsorption capacity of the amine group compounds impregnated solid sorbents (A-DETA, A-PEHA and A-PEI) presented a con-

tinuous increase with temperature from 298 K to 368 K due to the formation of carbamates which were formed between amines and CO_2 molecules as shown in Equation 5.3.

$$R_2NH + CO_2 \underset{\text{Heat}}{\overset{\text{Low temperature}}{\rightleftharpoons}} R_2NCOO^- + R_2NH_2^+ \quad (5.3)$$

The highest CO_2 adsorption capacity was observed for A-DETA over the range of temperature from 298 K to 368 K which was appropriated for the post combustion capture system.

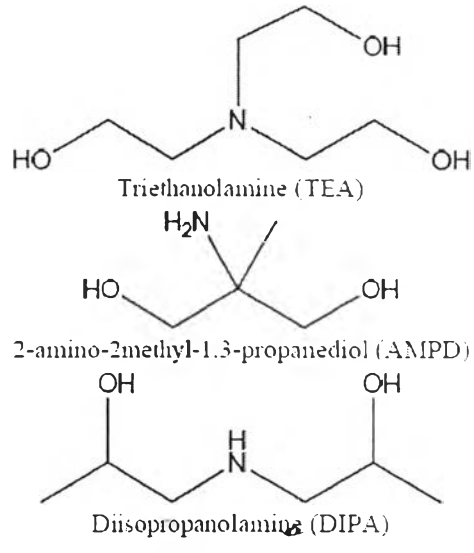

Figure 2.8 The structure of TEA, AMPD and DIPA (Yu *et al.*, 2012).

2.5.3 Polymer-based Compounds

Polymer is a chemical compound which composes of many repeating units, called monomer, and is synthesized from monomer molecules via polymerization process. These polymerization processes can be divided into two main types which are chain polymerization and step polymerization.

There are extensive researches on the development of adsorbent from polymer materials because these polymers perform many excellent properties, such as large surface area, high chemical stability, narrow pore size distribution, low skel-

eton density and much more functional groups, which can enhance the CO_2 adsorption performance.

The preparation of the triptycene based microporous polymer with pending tetrazole moieties (TMPT) which CO_2 capture from a mixture of the 9,10-dimethyl-2,3,6,7,12,13-hexahydroxytriptycene monomer, commercially available 2,3,5,6-tetrfluoroterephthalonitrile and pending tetrazole moieties via $ZnCl_2$ catalyzed post polymerization. The selectivity effect of adsorbed gases (CO_2, N_2 and CH_4) on the porous material was analyzed by volumetric adsorption apparatus at the same condition. The synthesized TMPT exhibited high selectivity towards CO_2 over N_2 and CH_4. The CO_2 adsorption capacity at 1.0 bar and 273 K was 5.98 mmol/ g due to the strong interactions between the electron rich in microporous polymer and CO_2 molecules. Moreover, the TMPT structure was not only suitable to adsorb CO_2 molecules, but also for H_2 molecules (Liu and Zhang, 2013).

The carbon dioxide capture and nanofiltration using microporous polyamide networks as adsorbent were studied by Qian *et al.* (2013). Firstly, the microporous polyamide networks were prepared from the interfacial polymerization of piperazine and acyl chloride monomers containing tetrahedral carbon and silicon cores with a yield of 90 - 92 %. These polyamides included tetraphenylmethane-chloride/piperazine (TPMC/PIP), tetra-phenylsilane-chloride/piperazine (TPSC/PIP) and trinesoyl chloride/piperazine (TMC/PIP). The results showed that the CO_2 uptakes at 1 bar and 273 K of TPMC/PIP, TPSC/PIP and TMC/PIP were 2.23, 1.95 and 0.41mmol/g, respectively, due to higher in surface area and micropore volume. These BET surface areas of TPMC/PIP, TPSC/PIP and TMC/PIP were 584, 488 and 105 m^2/g, respectively. The micropore volumes of TPMC/PIP, TPSC/PIP and TMC/PIP volumes were 0.357, 0.273 and 0.058 cm^3/g, respectively. These polyamides showed the CO_2/N_2 selective at 1 bar and 273 K due to a strong chemical interaction of CO_2 with amine groups. In case of the nanofiltration application, the TPMC/PIP, TPSC/PIP and TMC/PIP showed the salt rejection sequence of $FeCl_3$> $CaCl_2$>NaCl> Na_2SO_4.

A CO_2 adsorption with using guanidinylated poly(allylamina) supported on mesoporous silica foam as an adsorbent, which was prepared via a wet impregnation method (Alkhabbaz *et al.*, 2014). The organic loading effect of

poly(allylamina) (PAA) and guanidinylated poly(allylamina) (GPAA) impregnated sorbents indicated the same trend of CO_2 adsorption capacity. The CO_2 adsorption capacity increased with the increasing of organic loading and then dropped at a very high organic loading due to the pore blocking effect. The highest CO_2 adsorption capacity of PAA and GPAA impregnated sorbents was performed at 1.53 mmol CO_2/ g with 32 wt% of PPA loading and 1.38 mmol CO_2 /g with 35 wt% of GPAA loading, respectively, at 25 °C under dry condition using 10 % CO_2 in He. The effect of adsorption temperature showed that the PPA impregnated sorbent has higher CO_2 uptake than a GPPA impregnated sorbent at the temperature between 25–75 °C; whereas, the GPPA impregnated indicated higher CO_2 uptake than PPA impregnated above 75 °C because GPAA has guanidine groups in its structure that increased the basicity at high temperature. For a cycling performance, the CO_2 adsorption capacity of PAA and GPAA impregnated sorbents decreased by 5 % and 17 %, respectively, after five cycles at the temperature of 30 °C under dry condition using 10 % CO_2 in He.

2.6 Polybenzoxazine

One type of thermosetting polymer is polybenzoxazine which can be classified as a phenolic resin. A molecule of polybenzoxazine composes of an oxazine ring which is a heterocyclic six-membered ring with oxygen and nitrogen atom and it's affixed to a benzene ring (Ishida, 2011). Polybenzoxazine properties can be easily controlled to apply for different applications by adjusting the molecular structure during the curing process. Polybenzoxazine includes several preferential properties greater than the conventional phenolic resin as shown below:

- near-zero volume changes
- high thermal stability
- outstanding mechanical properties
- poor water absorption
- much higher glass transition temperature than the curing temperatures
- fast physical and mechanical property development
- very high char yield

- excellent electrical properties

A new type of phenolic material performs the potential properties to apply for various applications, moreover; it can be possible to be the alternate material for the existing polymers.

Benzoxazine resins can be classified into two types depending on the types of phenol used which are monofunctional and bifunctional types as shown in Figures 2.9 and 2.10.

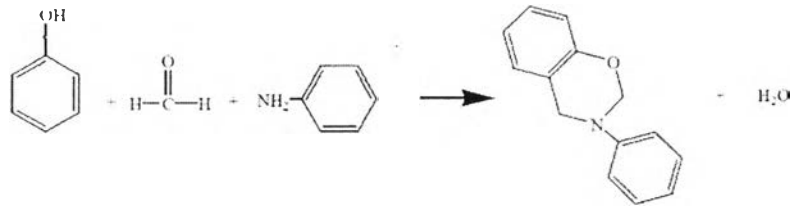

Figure 2.9 Monofunctional benzoxazine monomer synthesis (Lorjai *et al.*, 2009).

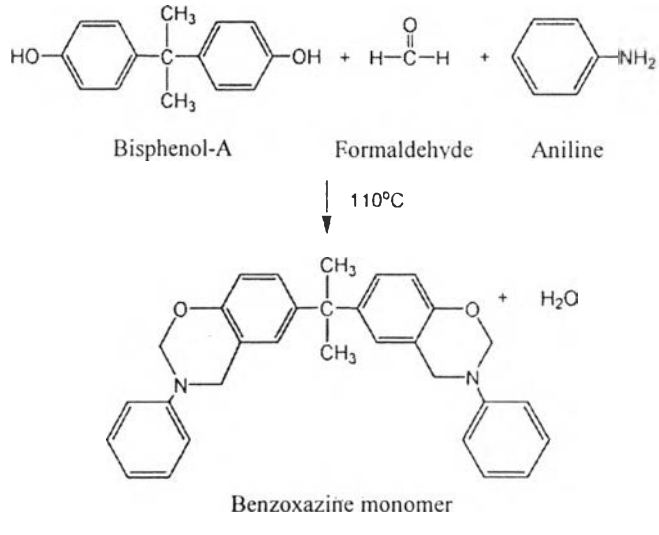

Figure 2.10 Bifunctional benzoxazine monomer synthesis (Lorjai *et al.*, 2009).

In the synthesis of polybenzoxazine typically three kinds of precursors are used, including phenols, formaldehyde, and amines. The reactions involve the ring

opening polymerization using heat for reaction process. The production of polybenzoxazine shows many benefits such as no by-products, no- purification process, no catalyst and, hence, leading to a production cost saving. In addition, the variation of molecular design flexibility depends on phenol and amine types. Currently, there are several researches who studied on the synthesis of polybenzoxazine for various applications.

The synthesis of fluorinated benzoxazine monomer was prepared by pouring 0.04 mol of 37 % formaldehyde solution with 5 ml dioxane in a three-necked round bottom flask under cool condition for 10 min. Then, 0.02 mol of aniline in 5 ml dioxane was poured in the flask by the slow dropping. After that, 0.01mol of hexafluoro bisphenol-A in 20 ml dioxane was poured and stirred. The mixture of three chemicals was reacted and refluxed at 100 °C for 24 hr. The solvent was removed in the rotary evaporator by reducing pressure and then the yellow solid product was obtained. The yellow solid product was dissolved in ethyl ether. Then, it was washed with 1 N NaOH and followed by water several times. After that, the solution product was dried with magnesium sodium and the solvent was removed in the rotary evaporator by reducing pressure. Finally, the light yellow solid product was obtained (Su and Chang, 2003).

The synthesis of polybenzoxazine aerogel via ring opening polymerization for removal of heavy metals from model wastewater was studied by Chaisuwan *et al.* (2010). The benzoxazine precursor was prepared from bisphenol-A (4.52 g), formaldehyde (6.48 g) and triethylenetetraamine (2.92 g), with a molar ratio of 1:4:1, in dioxane (20 ml) and the viscous liquid of benzoxazine precursor was obtained. Then, it was mixed and heated at 80 °C for 72 h followed by solvent evaporation. After that, the samples was fully cured at 140 °C, 160 °C and 180 °C for 2 h at each temperature and then at 200 °C for 3 h. The results showed that the pore size distribution of the polybenzoxazine based aerogel was performed around 2 nm and the order of metal ions removal was in the following of Sn^{2+}> Cu^{2+}> Fe^{2+}> Pb^{2+}> Ni^{2+}> Cd^{2+}> Cr^{2+} due to the Trving- Williams rule.

In the previous study, the polybenzoxazine-derived activated carbons synthesized from phenol, formaldehyde and diethylenetriamine (DETA) as precursors had been studied. The results revealed that the CO_2 adsorption capacity of AC-DETA

at carbonization temperature of 200, 300 and 400 °C were 1.58, 1.65 and 1.59 mmol/g, respectively, and it performed higher CO_2 adsorption performance than the commercial activated carbon (1.50 mmol/g) at 40 °C and 1 bar due to the high amount of nitrogen functionalities. However, the textural parameters were displeasing in term of low surface area at 267 m^2/g and low total pore volume at 0.30 cm^3/g for AC-DETA at carbonization temperature of 300 °C (Hirikamol, 2013).

In the present study, the improvement of textural parameters is become interesting because the high potential surface area can enhance the CO_2 adsorption capacity in term of increasing the nitrogen surface functionalities. Therefore, there are two techniques to increase the surface area and porosity in polybenzoxazine.

2.6.1 Foaming Technique

Polymeric foam can be classified as a two phase material including with dispersed phase of gas in a continuous phase of polymer matrix. This material is significant in term of its high strength to weight ratio. Moreover, there are many advantages such as the chemical resistance, cushioning performance, shock absorption and thermal insulation. The most popular polymeric foams are polyurethane (PU), polystyrene (PS), and polyethylene (PE) foam. The foam structure can be produced by using a blowing agent. The foaming agents can be divided into two classes which are chemical blowing agent (CBA) and physical blowing agent (PBA) (Zúñiga *et al.*, 2012). For the CBA, this blowing agent generates gases from a chemical reaction. For the PBA, it generates gases from a physical process such as evaporation, increasing temperature or decreasing pressure, using nitrogen, carbon dioxide, and hydrocarbons. However, there are limited researches on the synthetic polybenzoxazine foam due to a new class of material.

The synthesizes of polybenzoxazine foam and carbon foam were also studied by Lorjai *et al.* (2009). In their work, the polybenzoxazine foam was prepared from bisphenol-A, aniline and para- formaldehyde with the mole ratio of 1:2:4. Then, it was mixed and heated at 110 °C for 60 min to obtain benzoxazine monomer. After that, it was mixed with azodicarbonamide (1, 3, 5, 7 and 10 wt%) at 110 °C and was cured from 30 °C – 210 °C at 1°C/min. Finally, the polybenzoxazine foam was obtained. In case of the synthesis of carbon foam, it was carbonized under nitro-

gen flow at 500 cm^3/min, using the following temperature program: 30 – 250 °C in 60 min, 250 – 600 °C in 300 min, 600 – 800 °C in 60 min and holding at 800 °C for 60 min. Then, the carbon foam was obtained. The result of polybenzoxazine foam showed that compressive modulus and compressive strength increased as the foam density increased and the pore distribution was smaller and more uniform after the polybenzoxazine foam was carbonized. The microscopic images of polybenzoxazine foam and carbon foam were shown in Figure 2.11. After carbonization, compressive modulus and compressive strength increased due to the decrease of foam density.

The synthesis of polybenzoxazine foam using azodicarbonamide (ADC) as a blowing agent was studied by Ardanuy *et al.* (2012). In their work, the polybenzoxazine foam was prepared from benzoxazine resin based on bisphenol-A derivative. First, the benzoxazine resin was heated at 150 °C for 30 min and mixed with 5 wt% of ADC. Then, it was cured from 150 °C to 200 °C at 2.5 °C/ min and was held at 200 °C for 80 min. They studied the polybenzoxazine with differences of relative densities at 0.35, 0.43, 0.50 and 0.60. The results showed that compressive strength, compressive modulus and cell size were performed in the ranges of 10–70 MPa and 400–1100 MPa and 499–159 μm, respectively. The microscopic images of polybenzoxazine foams with the different relative densities were shown in Figure 2.12.

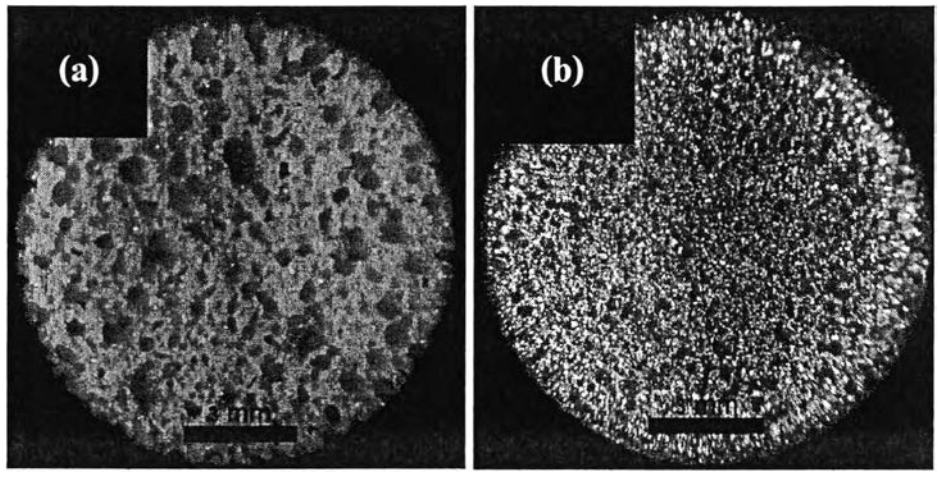

Figure 2.11 The microscopic images of polybenzoxazine foam (a) and carbon foam (b) at 10 wt% of AZD (Lorjai *et al.*, 2009).

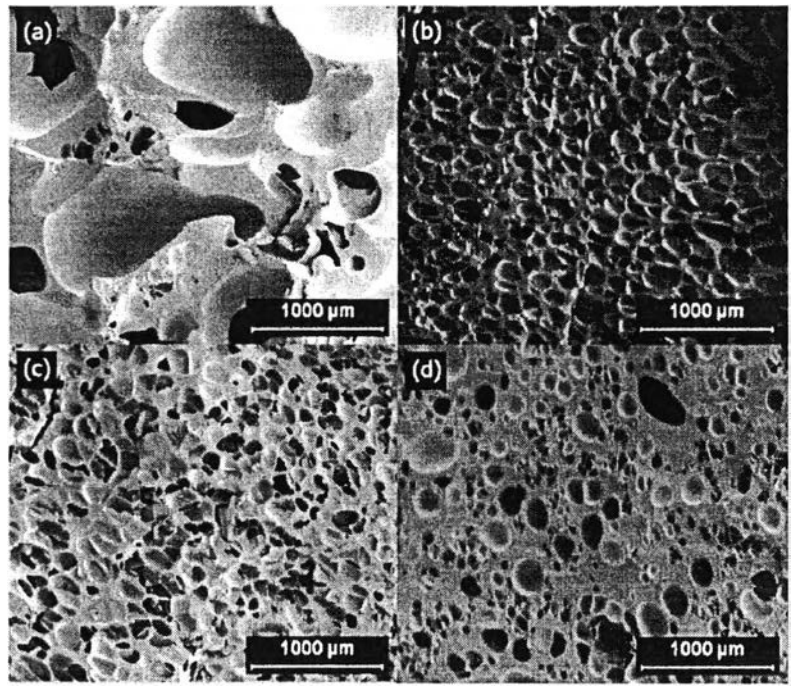

Figure 2.12 The microscopic images of polybenzoxazine foams at several relative densities (a) 0.35, (b) 0.43, (c) 0.50 and (d) 0.60 (Ardanuy *et al.*, 2012).

The preparation of the diphenolic acid benzoxazine (DPA-Bz) foam via self-foaming process was studied by Zúñiga *et al.* (2012). First, diphenolic acid benzoxazine was heated at 140 °C for 30 min and compress in steel mold. Then, it was partially cured at 140 °C for 6 h and 160 °C for 2 h. After that, it was fully cured from 30 °C to vary temperatures of 190, 200, 210, 220 and 230 °C at 3.5 °C /min. This method could generate CO_2 gases within the polymer to form a foam structure via decarboxylation reaction. The result showed that the cell sizes at foaming temperatures of 190, 200, 210, 220 and 230 °C performed at 69.0, 101.5, 118.7, 136.5 and 146.1 µm, respectively, and high foaming temperature indicated a high value of cell size because this temperature performed a high CO_2 pressure inside the bubble. The microscopic image of diphenolic acid benzoxazine foam was shown in Figure 2.14.

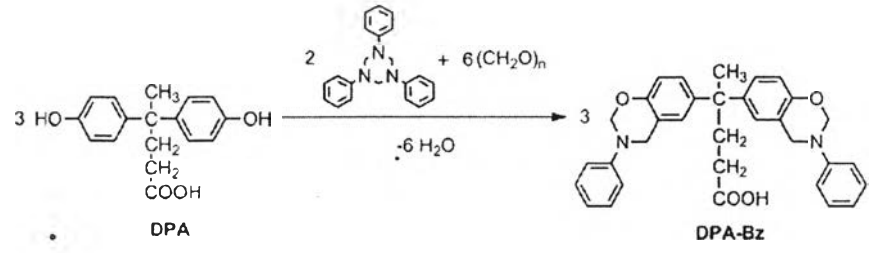

Figure 2.13 Synthesis of diphenolic acid benzoxazine (Zúñiga *et al.*, 2012).

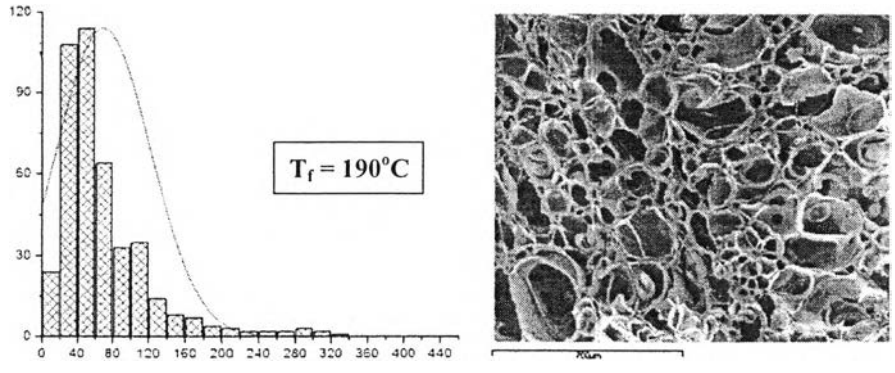

Figure 2.14 Cell size distribution and microscopic image of diphenolic acid benzoxazine foam at foaming temperature of 190 °C (Zúñiga *et al.*, 2012).

Table 2.6 The synthesis and pore size diameter of polybenzoxazine foam

Polybenzoxazine Precursors (Molar Ratio)	Foaming Agent	Condition	Pore Size	
1. Diphenolic acid (DPA) 2. Ammonium sulphate 3. Para-formaldehyde (3:2:6) (Zúñiga *et al.*, 2012)	Not require (Self-foaming diphenolic acid benzoxazine, DPA-Bz)	- DPA-Bz was heated at 140 °C for 30 min and compress in steel mould. - Be partially cured at 140 °C for 6 h and at 160 °C for 2 h. - Be fully cured from 30 °C to vary temp. (190, 200, 210, 220 and 230 °C) at 3.5 °C/min.	T_f (°C)	Cell Size (μm)
			190	69.0
			200	101.5
			210	118.7
			220	136.5
			230	146.1
			T_f = foaming temperature	

Table 2.6 The synthesis and pore size diameter of polybenzoxazine foam (Con't.)

Polybenzoxazine Precursors (Molar Ratio)	Foaming Agent	Condition	Pore Size	
1. Bisphenol-A 2. Anlline 3. Para-formaldehyde (1:2:4) (Lorjai *et al.*, 2009)	AZD (azodicarbon-amide)	- Mixed and heat at 110 °C for 60 min to obtain monomer. - Mixed with AZD (1, 3, 5, 7 & 10 wt%) at 110 °C. -cured from 30 – 210 °C at 1 °C/min.	-Large pore in mm unit	
Benzoxazine resin (based on bisphenol-A derivative) (Ardanuy *et al.*, 2012)	ADC (azodicarbona-mide)	- Bezoxazineresin was heated at 150 °C for 30 min and mixed with ADC (5 wt%). - Cured from 150 – 200 °C at 2.5°C/min and hold at 200 °C for 80 min.	Sample	Cell Size (μm)
			B-ADC$_{0.35}$*	499
			B-ADC$_{0.43}$*	188
			B-ADC$_{0.50}$*	119
			B-ADC$_{0.60}$*	159
			*relative density	

In this work, a sol-gel technique is attended to design the suitable adsorbent structure for CO_2 capture application.

2.6.2 A Sol-gel Technique

The synthesis of polybenzoxazine based carbon aerogel electrode for supercapacitors was studied by Katanyoota *et al.* (2010). Two types of polybenzoxazines from two different amines were synthesized which are aniline and triethylenetetramine. First case of BA-teta, the synthesis of benzoxazine precursor was prepared from bisphenol-A, triethyleneteramine and para-formaldehyde, with a molar ratio of 1:1:4, in dioxane by using a quasi solventless method. Then, the yellow viscous liquid was obtained. After that, it was mixed and heated at 80 °C for 72 h and was cured at 160 °C and 180 °C for 3 h at each temperature and 200 °C for 2 h. Second case of BA-a, the synthesis of benzoxazine precursor was prepared from bisphenol-A, aniline, para- formaldehyde, with a molar ratio of 1:2:4, via a solventless method. Then,

the yellow viscous liquid was obtained. After that, it was mixed and heated at 110 °C for an hour and was partially cured at 130 °C for 96 h. Finally, it was fully cured at 160 °C and 180 °C for an hour at each temperature and 200 °C for 2 h. The carbon aerogel of each polybenzoxazine was prepared by pyrolyzed at 30-250 °C in 60 min, 250–600 °C in 300 min, 600–800 °C in 60 min and held at 800 °C for 60 min. The result showed that the average pore size, BET surface area and total pore volume of BA-teta was 3.67 nm, 368 m^2/g and 0.34 cm^2/g, respectively, and the average pore size, BET surface area and total pore volume of BA-a was 2.20 nm, 391 m^2/g and 0.21 cm^2/g, respectively. For supercapacitor application, a specific capacitance of BA-teta and BA-a were 55.78 and 20.53 F/g, respectively.

The synthesis of bisphenol-A/aniline based polybenzoxazine aerogel for enhancement of thermal stability in the non-oxidative thermal degradation was studied by Lorjai *et al.* (2011). The polybenzoxazine was prepared from bisphenol-A, aniline and para- formaldehyde with a molar ratio of 1:1:4. Then, it was mixed and heated at 110 °C for 60 min to obtain yellow color of monomer. After that, monomer was cured at 160 °C and 180 °C for an hour at each temperature and finally at 200 °C to obtain bulk polybenzoxazine. The polybenzoxazine aerogel was prepared by mixed monomer (40 %) with xylene and heated at 130 °C for 96 h. Then, it was fully cured same step with bulk polybenzoxazine to obtain aerogel. The result showed that the pore size of polybenzoxazine aerogel was performed in micrometer length with uniform porous and polybenzoxazine aerogel exhibited higher degradation temperature and char yield than bulk polybenzoxazine.

2.6.2.1 Porous Carbon Containing Non-ionic Surfactant

Polybenzoxazine-based carbon xerogels loading with surfactant were studied by the research of Thubsuang (2015). These carbon xerogels were compared to study the effect of surfactant types, namely cationic (CTAB) and non-ionic surfactants (Synperonic NP30), on the porous PBZ-based carbon xerogels. Moreover, the influence of surfactant content on carbon xerogels was varied in order to alter their surface properties. The results showed that carbon xerogels with cationic surfactant generated porosity in the mesoporous range and provided the form of nano-spherical particles with approximately 100 nm in size. Besides, the increasing of cationic surfactant concentration led to a decrease in mesopore diameter from 35

Table 2.7 The synthesis and pore size diameter of porous polybenzoxazine

Polybenzoxazine Precursors (Molar Ratio)	Porous Material	Condition	Pore Size
1. Bisphenol-A 2. Triethylenetetramine 3. Formaldehyde (1:2:4) (Chaisuwan *et al.*, 2010)	Polybenzoxazine aerogel	- Be mixed and heated at 80 °C for 72 h followed by evaporating solvent. - Be fully cured at 140, 160 and 180 °C for 2 h at each and then at 200 °C for 3 h.	- Average pore diameter at 2 nm.
1. Bisphenol-A 2. Aniline 3. Para-formaldehyde (1:2:4) (Lorjai *et al.*, 2011)	Polybenzoxazine aerogel	- Be mixed and heated at 110 °C for 60 min to obtain monomer. - Cured at 160 and 180 °C for an hour at each and finally at 200 °C to obtain bulk polybenzoxazine. - Be mixed monomer (40 wt%) with xylene and heated at 130 °C for 96 h - Fully cured same step with bulk polybenzoxazine to obtain aerogel.	- Pore size in micrometer length with uniform porous.
Case I (BA-teta) 1. Bisphenol-A 2. Triethylenetetramine, 3. Para-formaldehyde (1:1:4) **Case II (BA-a)** 1. Bisphenol-A 2. Aniline 3. Para-formaldehyde (1:2:4) (Katanyoota *et al.*, 2010)	Carbon aerogel	**Case I** - Be mixed and heated at 80 °C for 72 h. - Be cured at 160 and 180 °C for 3 h at each and 200 °C for 2 h. **Case II** - Be mixed and heated at 110 °C for an hour. - Be partially cured at 130 °C for 96 h. - Be fully cured at 160 and 180 °C for an hour at each and 200 °C for 2 h. *For each case - Be pyrolyzed at 30-250 °C in 60 min, 250 – 600 °C in 300 min, 600-800 °C in 60 min and held at 800 °C for 60 min	**CA(BA-teta)** / **CA(BA-a)** *Average pore size (nm)* 3.67 / 2.20 *Mesoporosity (%)* 62 / 23 *BET (m^2/g)* 368 / 391 *Total pore volume (cm^3/g)* 0.34 / 0.21 *Micropore volume (cm^3/g)* 0.13 / 0.17 *Mesopore volume (cm^3/g)* 0.21 / 0.05

to 15 nm for carbon xerogels with CTAB concentrations of 0.003 and 0.180 M, respectively. Conversely, the results from carbon xerogels with Synperonic NP30 indicated that the loading non-ionic surfactant on carbon xerogel caused the shifted in the

pore characteristics from mesoporous material (original carbon xerogel) to microporous material (carbon xerogels with 0.180 M of Synperonic NP30).

Another porous carbon material containing non-ionic surfactant was studies in the work of Wang *et al.* (2011). This study was about the preparation of carbon aerogel-based microspheres via inverse emulsion polymerization. In particular, the influences of stirring speed and loading of surfactant (SPAN80) on carbon microspheres were investigated; moreover, these materials were used as carbon electrodes for the application of supercapacitor. In case of the stirring speed, at high speed used (720 rpm), the carbon particles were smaller compared to the carbon aerogels prepared at low stirring speed and provided the spherical diameter of 2 μm. For the effect of loading surfactant on carbon aerogel microspheres, when the concentration of non-ionic surfactant was increased from 0.01 to 0.05 ($V_{surfactant}$/ $V_{hexamethylene}$), the average pore size of carbon aerogel microspheres was decreased from 4.95 to1.43 nm. In addition, the surface areas (or mesopore volumes) of CA microspheres at 0.01, 0.02, and 0.05 were 603 (0.432), 533 (0.260), and 414 m^2/g (0.028 cm^3/g), respectively. On top of that, the highest capacitance of electrode was observed for CA microspheres prepared at V_s/V_h = 0.01 and the stirring speed of 480 rpm which exhibited the value up to 180 F/g.

2.7 Adsorption Measurement

There are several methods used to measure the adsorption capacity of the adsorbents such as gravimetric, volumetric and temperature programmed desorption (TPD).

2.7.1 Gravimetric Method

This method carries out using 1- 10 mg of sample for measuring the adsorption capacity. It is sensitive for all gas that was adsorbed on an adsorbent and the error of adsorption capacity is observed when the impurities are composed of 0.01 mg or 1 wt%.Therefore, the gravimetric method is suitable for an adsorbent with high adsorption capacity (Blackman *et al.*, 2006).

2.7.2 Temperature Programmed Desorption (TPD)

This method was carried out using 1- 10 mg of sample for measuring the adsorption capacity and the temperature was controlled in the ranges of 90- 970 K under ultra-high vacuum pressure (ca. 10^{-6} Pa). This method measures the adsorbed molecules by mass spectrometry which calculates the amount of molecules from the desorption process (Blackman *et al.*, 2006).

2.7.3 Volumetric Method

The adsorption capacity is determined by measuring the pressure drop after CO_2 molecules are adsorbed onto the adsorbent at constant volume. For the basic concept of volumetric method, this method is composed of a reservoir and a sample cell. First, the sample is placed in a sample cell. Then, the reservoir and the sample cell are degased and then the reservoir is isolated. After that, the reservoir is filled with CO_2 molecules and the CO_2 molecules are expanded to the sample cell. Finally, the CO_2 adsorption capacity is calculated. The schematic of the volumetric differential pressure hydrogen adsorption apparatus is shown in Figure 2.15 (Blackman *et al.*, 2006).

The adsorption capacities were investigated by volumetric adsorption apparatus. The operating pressure of the apparatus was applied at 10 MPa. This method required a limitation at 0.1 wt% and accuracy at 0.05 wt%. The temperature was kept constant at 30 ± 0.1 °C. The volumes of the reservoirs (R1 and R2) and the sample cells are 168.1 ml and 17.3 ml, respectively. After hydrogen was filled in the reservoirs, hydrogen was expanded from the reservoirs to the samples and then it was returned to the equilibrium. After that, the hydrogen storage capacity was determined by using a differential pressure between a reference cell and sample cell. The result showed that the amount of hydrogen adsorbed was less than 1 wt% for all the carbons examined (Blackman *et al.*, 2006).

The volumetric method has many benefits such as to be more accuracy in term of the pressure monitoring and to avoid the effect of non-ideal gas expansion. In addition, this method uses large quantity of sample (1.0 – 2.5 g) and uses a helium baseline correction, since they lead to eliminate large errors and to perform an accuracy result. Therefore, the in-house volumetric sorption apparatus is devel-

oped for determining the CO_2 adsorption performance of adsorbent. Moreover, the pressures will be monitored and recorded from the beginning of adsorption measurement until the equilibrium is reached and referred to as adsorption isotherm and will be used to determine the CO_2 adsorption capacity.

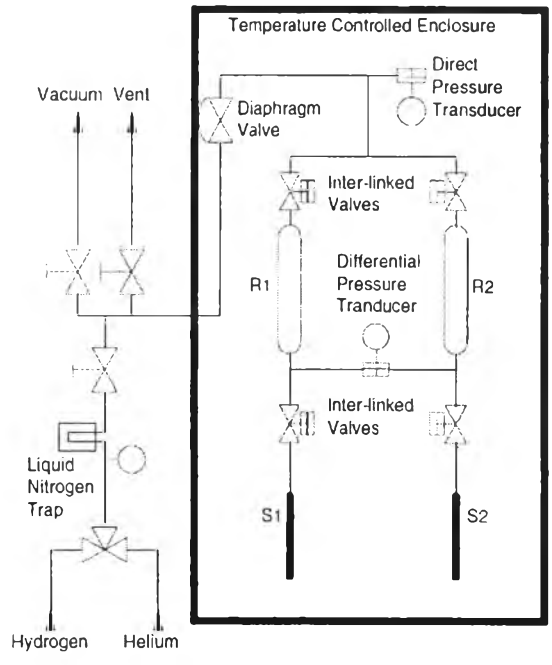

Figure 2.15 Schematic of the volumetric differential pressure hydrogen adsorption apparatus (Blackman *et al.*, 2006).

MOTIVATION

Polybenzoxazine is a new type of phenolic resin and easily synthesized via ring opening polymerization. It reveals prominent characteristics for CO_2 capture in terms of the good mechanical properties, high thermal stability, low water absorption, etc., hence, it is a promising material as adsorbent for CO_2 capture. Amine groups embedded in the structure of polybenzoxazine are ready to act as basic molecules and interact with acidic CO_2 molecules. In previous work, the polybenzoxa-

zine-derived activated carbon was evaluated as a potential source of basic sites for CO_2 capture. A CO_2 adsorption capacity of 1.65 mmol/g was obtained from the polybenzoxazine-derived activated carbon synthesized from phenol, formaldehyde and DETA as precursors (Hirikamol, 2013). Nevertheless, the surface area of the resulted carbon was too low, i.e. 267 m^2/g after 1-hr carbonization at 300 °C and 1-hr CO_2 activation at 800 °C. In the present study, it is of interest to increase the surface area and create interconnected pores in polybenzoxazine from these precursors by using a sol-gel technique.

HYPOTHESIS

Phenol-based polybenzoxazines from two different types of amine precursors (e.g., DETA and PEHA) will be synthesized. Since the different chain lengths of amine precursor may create different pore size of polybenzoxazine after carbonization. It is hypothesized that a shorter chain length of amine precursor would create polybenzoxazine with smaller pore sizes in the microporous range. To increase the surface area and porosity in the adsorbent structure, the sol-gel technique is used. Since the benzoxazine content affects directly to the void size within the solid skeleton after the solvent removal, it is of interest to study the effect of benzoxazine content to the generation of porosity in polybenzoxazine aerogels. It is hypothesized that the higher the benzoxazine content, the higher the porosity in microporous ranges would be create. In addition, loading non-ionic surfactant in aerogel materials may help generate more porosity within the structure of polybenzoxazine during the sol-gel preparation method. It is hypothesized that adding a small amount of non-ionic surfactant in PBZ-based aerogels could improve their surface properties.

The objectives of this study are as followed as:

1. To compare the pore size of carbonized polybenzoxazine derived from amine precursors with different chain length.
2. To increase the surface area and porosity of polybenzoxazine-based carbon aerogel by using a sol-gel technique.
3. To improve a capability for controlling the porosity on polybenzoxazine-based carbon aerogel by adding a non-ionic surfactant.

4. To compare the effect of CO_2 adsorption between two different types of polybenzoxazine-based carbon aerogels.

The scope of this research will cover the following:

Objective 1:

- In the present study, the two different types of polybenzoxazines were synthesized from phenol, formaldehyde and two different amine precursors that were diethylenetriamine (DETA) and pentaethylenehexamine (PEHA).
- The influence of amines with different chain lengths on the pore size of polybenzoxazine.

Objective 2:

- The porous polybenzoxazine was prepared by using a sol-gel technique in order to increase the surface area and the porosity of polybenzoxazine aerogel.
- The benzoxazine content in the reaction mixture was varied to study the change in porosity of the polybenzoxazine aerogels.
- The porous carbon was prepared via carbonization and activation processes.
- The porous polybenzoxazine-based carbon aerogel was characterized to determine the microporous and mesoporous ranges before and after the carbonization and activation step.

Objective 3:

- In this study, PEG-PPG-PEG block copolymer was used as a non-ionic surfactant and fixed at 6 wt%.
- The influence of loading of non-ionic surfactant in PBZ-based carbon aerogels on their textural properties was studied.

Objective 4:

- The effect of polybenzoxazine preparation variables (i.e. different amine precursors, benzoxazine content, carbonization and activation) on the CO_2 adsorption performance was studied.

- The effect of surface morphology (using BET surface area analyzer and SEM), surface functionalities (using TGA-FTIR, XPS and CHN) and other adsorbent properties (using TGA, DSC and gas pycnometer) on CO_2 adsorption performance were studied to relate these properties to the polybenzoxazine preparation variables.
- The effect of temperature and pressure of the adsorption and desorption process was studied to find out the suitable adsorption condition.